Proc Indian Natn Sci Acad, **70, A,** No. 3, May 2004, pp. 483-488

ELECTROCHEMICAL INVESTIGATIONS OF OXIDE COATED NANOPARTICLES

V SURYANARAYANAN, RENJIS T TOM, A SREEKUMARAN NAIR AND T PRADEEP*

Department of Chemistry and Sophisticated Analytical Instrument Facility, Indian Institute of Technology Madras, Chennai-600 036 (India)

(Received 30 November 2002; Accepted 24 March 2003)

Titania and zirconia covered Au and Ag nanoparticles ($Au@TiO_2$, $Au@ZrO_2$, $Ag@TiO_2$ and $Ag@ZrO_2$) with controllable shell thickness have been prepared by one pot synthesis and characterized by a variety of techniques; the focus of this paper is cyclic voltammetry (CV). High reactivity of Ag nanoparticles towards halocarbons leads to the destruction of the metal core, which was monitored by the decay in the oxidation and reduction current of the Ag_n/Ag_n^+ couple. The study shows that the oxide shell is porous for ion transport. An attempt was made to synthesize oxide coated alloy nanoparticles of different compositions of Au and Ag.

Key Words : Nanoparticles; Core-Shell Nanosystems; Optical Spectroscopy; Electrochemistry; Nanochemistry; Plasmon Resonance

Introduction

Nanosize materials are important in present day research, especially in areas such as semiconductors[1]. Materials in the nanometer range with well-defined (atomic/molecular) structures are expected to exhibit functional properties for a wide range of technological applications - including catalysis, optics, microelectronics and chemical/biological sensors[2-5]. The electrical, optical and catalytic properties depend on the characteristic dimension of the structural units, which is in the range of 1-100 nm[6]. As far as metal nanoclusters are concerned, the resonance frequency and width of the plasmon absorption band depend on the nanoparticle size, shape and distribution[7]. Due to their extreme reactivity in the free state, metal nanoparticles have to be coated with either monolayers or with inert compounds such as oxides or polymers to preserve their identity. Coating of a thin layer of metal oxide over the nanoparticle makes it possible to control inter-particle and particle-matrix interactions, thereby improving functional properties of devices, thus expanding the range of potential applications. Some of the examples are silica[8], titania[9] and zirconia[10] covered noble metal clusters.

Chlorofluorocarbons (CFCs), the working fluids used in refrigerators for cooling, are some of the important pollutants which cause major destruction to the ozone layer. Several approaches have already been developed for the destruction of these CFCs[11-13], which also include the use of metal nanomaterials. One of the most recent approaches in this direction is the reaction, $2CuO + CCl_4 \rightarrow 2CuCl_2 + CO_2$, using metal oxide nanoparticles[14]. We have found that halocarbons react with metallic nano particles forming halide ions and amorphous carbon; the process can be viewed as metal oxidation with catalytic destruction of CFCs. The reaction is efficient and ecofriendly and the metal ions formed can be recycled completely. This reaction, when used for core-shell nanomaterials, could generate oxide nanobubbles.

In this article, we describe the electrochemical investigation of TiO_2 and ZrO_2 covered Au and Ag metal nanoparticles. Studies include the formation of the oxide shells over metal nanoparticles and the destruction of core using halocarbons. Characterization of these nanomaterials was done by UV-visible spectrophotometry, cyclic voltammetry (CV) and transmission electron microscopy (TEM). Limited work was carried out to identify different compositions of nanoalloys containing both Ag and Au.

Experimental Section

Zirconium (1V) propoxide and titanium tertiary butoxide were obtained from Aldrich. $AgNO_3$ and $HAuCl_4$ were purchased from Qualigens chemicals, India. All the

*Author for Correspondence :
E-mail: pradeep@iitm.ac.in *Fax:* ++91-44-257 0509/0545

other chemicals used in the experiments were from local sources and he solvents were distilled prior to use. Zirconia covered silver nanoparticles were prepared by one-pot synthesis. Preparation $Ag@ZrO_2$ involves the formation of silver core and coating of the oxide cover. The silver nanoparticles are formed by the reduction of Ag^+ using DMF as per the reaction[10(a), 10(b), 18],

$$HCONMe_2 + 2Ag^+ + H_2O \rightarrow 2Ag^0 + Me_2NCOOH + 2H^+ \quad ...(1)$$

The formed carbamic acid will be easily decomposed to carbon dioxide and dimethyl amine (Me_2NH). 30 mg of $AgNO_3$ was dissolved in a mixture of 15 ml dimethylformamide (DMF) and 5 ml H_2O. Another solution containing 200 µl of acetyl acetone and 250 µl of zirconium (1V) propoxide in 40 ml of 2-propanol was prepared. The two solutions were mixed and refluxed for 45 minutes at 90 °C till a greenish-black colour appeared. This solution consists of core shell particles of ~30-60 nm core diameter and ~3 nm shell thickness. The solution became pink in the case of Au and green-black in the case of Ag. The colour change during synthesis was abrupt in the case of Au and more gradual in the case of Ag. Further refluxing of the solution led to the formation of a precipitate, which could be dispersed by sonication. The procedure for the synthesis of the alloy material is the same as above except that different amounts of $AgNO_3$ and $HAuCl_4$ were taken, according to the composition, instead of a single component.

UV-visible spectra were measured with a Varian Cary 5 UV/VIS/NIR spectrophotometer and a Perkin Elmer Lambda 5 spectrometer. Transmission electron microscopy (TEM) measurements were performed with a Philips CM12 microscope working at 120 KeV acceleration. The sample solution was drop-casted on carbon coated copper grids. Cyclic voltammograms were obtained on an electrochemical analyzer (CH Instruments model 600A) in a standard three-electrode cell comprising of a Pt disk (area = 0.8 mm^2) as working electrode, platinum foil as counter electrode and Ag/AgCl as reference electrode. Voltammetry was performed at various scan rates in acetonitrile containing 0.1 M tetrabutylammonium hexafluorophosphate ($TBAPF_6$) as supporting electrolyte. For recording CV, 4 ml of the cluster solution was dissolved in 10 ml of the supporting electrolyte solution.

Results and Discussion

Metal nanoparticles have very intense and characteristic colour which gives rise to surface plasmon absorption in UV-Visible spectroscopy. There are some shifts in the plasmon resonance of Ag and Au from their characteristic values upon encapsulation with oxide cover; there are also changes in the peak position depending on the thickness of the shell and the particle dimension. The shift from the free metal particle may be attributed to the dielectric constant of the surrounding matrix upon encapsulation[9]. For example, the values for the characteristic surface plasmon absorption for ZrO_2 covered Ag and Au nanoparticles are 425 and 531 nm, respectively with the same particle size (Fig. 1) and the shift can be explained by Mie's theory[15].

The average shell thickness observed in all the cases under this condition is in the range of 2- 3 nm. With increasing shell thickness, the plasmon band red shifts and the width of the peak increases. This can be achieved by increasing the concentration of the oxide precursor and hydrolysis time. The increase in the reaction time allows hydrolysis to occur to a greater extent over the particles. The peak width also increases with dimension of the core in this size range.

A dilute solution of the particles was dropped onto carbon coated TEM grids and micrographs were taken. The TEM pictures are shown in Fig. 2. A

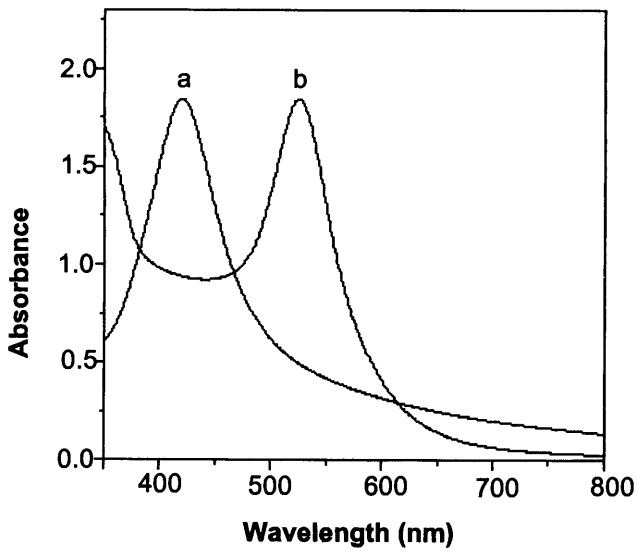

Fig. 1 UV-Visible spectra of zirconium oxide coated a) silver and b) gold nanoparticles.

collection of ZrO_2 covered silver particles with absorption maximum of 425 nm are shown in Fig. 2A. There are particles in the size range of 30 – 60 nm. Although most of the particles are spherical, faceted structures are also evident. In picture 2B, close-up view of one core-shell structure of $Ag@ZrO_2$ is shown where the presence of the core as well as the shell is clear. Though the particles have different core thickness, the shell thickness is in the range of 2-3 nm and is uniform. By changing other conditions such as temperature and concentration of the salt solution, it must be possible to get smaller core sizes. TiO_2 coated Au and Ag particles were also prepared and studied, which had similar thicknesses and particle sizes.

These oxide-covered nanomaterials have been investigated for their electrochemical behaviour in solution phase on Pt electrodes. Typical CV of zirconia coated Ag nanoparticles in the CH_3CN/ TBAHFP solvent-supporting electrolyte system at a constant sweep rate of 0.3 Vs^{-1} is shown in Fig. 3A. In the anodic direction from 0 V to 0.6 V, $Ag@ZrO_2$ shows one characteristic anodic peak at 0.310 V and a cathodic peak at 0.120 V. CV shows the redox couple centered at $E_{1/2}$ = 0.195 V Vs Ag/ AgCl with a peak separation ΔE_p of 170 mV for anodic peak (Fig. 3A). In an earlier work related to dodecanethiol capped silver nanoclusters, the observed cathodic peak potential was around 0.242 V with an $E_{1/2}$ value of 0.128 V Vs Ag/AgCl and the peak separation ΔE_p was 0.229 V[16]. A comparison of the studies reveals that the peak potential is shifted to more positive value in the case of zirconia coated metal clusters. The quasi-reversible peaks corresponding to the oxidation and reduction of Ag clusters can be represented as,

$$Ag_n \rightarrow Ag_n^+ + e \qquad ...(2)$$

The surface coverage calculated from the area under the anodic peak is found to be larger than the cathodic peak, which results in higher anodic currents during scanning. During the potential cycling, the peak currents for both the anodic and the cathodic regions are found to increase with cycling and this may be associated with the possibility of silver deposition on Pt electrode. The peak potential and peak currents also vary linearly with scan rate.

From the above studies, it is observed that silver clusters, though coated with a zirconium oxide shell, are still accessible to electron transfer by the applied potential in CV; note that totally passivated clusters are not expected to show any redox behaviour. This

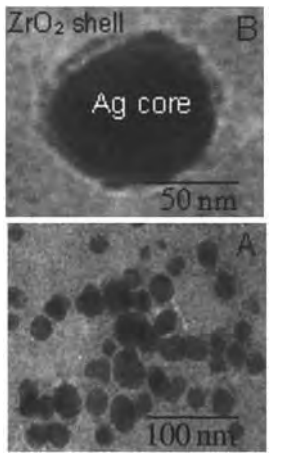

Fig. 2 Transmission electron micrographs of ZrO_2 covered Ag nanoparticles. *A* represents a larger view and *B* is a close-up of one $Ag@ZrO_2$ particle. The core and the shell are clearly seen.

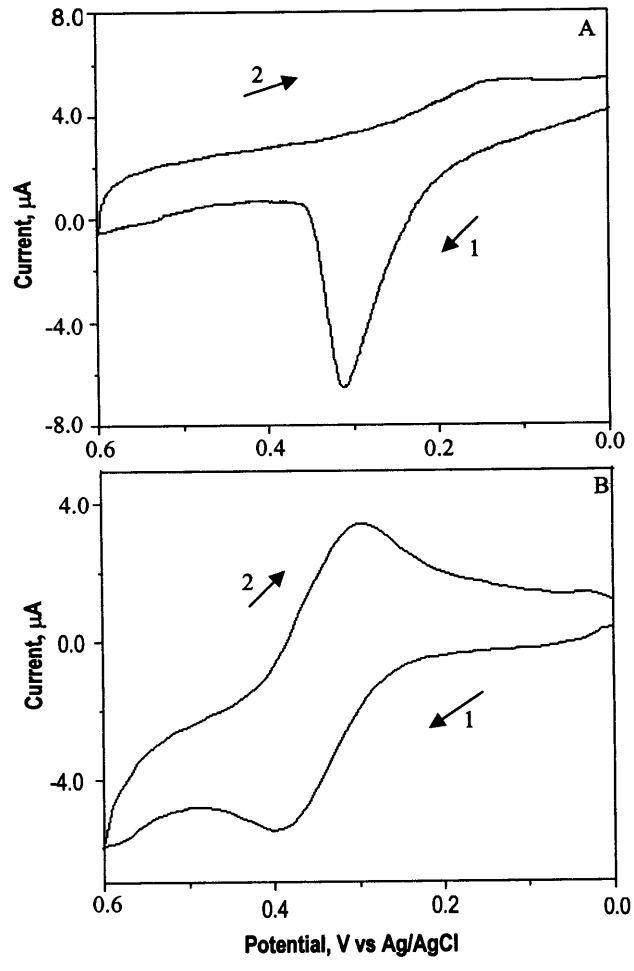

Fig. 3 Cyclic voltammogram of (A) $Ag@ZrO_2$ and (B) $Au@TiO_2$ on Pt electrode in CH_3CN containing 0.1 M tetrabutyl ammonium hexafluorophosphate at a constant sweep rate of 0.3 Vs^{-1}.

confirms the porous nature of the oxide shell. Similarly, reduction and oxidation of Au_n/Au^+_n couple is also observed for $Au@TiO_2$ nanomaterial. The voltammetric response of the above material at the same sweep rate is shown in the Fig. 3B for comparison. The anodic peak is at 0.394 V and cathodic peak is at 0.310 V (Fig. 3B). The peak current ratio of reduction and oxidation of this couple is approximately equal to 1, representing a simple reversible one-electron transfer reaction. It is also noted that above nanoparticles covered with either TiO_2 or ZrO_2 do not have much difference in their peak potential values.

These nano cores are very reactive through the pores of the oxide matrix. The reactions studied with halocarbons cause the destruction of the core, leaving behind the shell. The time dependent UV-visible spectra of $Ag@ZrO_2$ reaction with 50 µl of benzyl chloride are shown in Fig. 4. The intensity of the plasmon absorption band decreases with time, which implies selective leaching of the Ag core. Finally, the absorption plasmon of the nanomaterial disappears resulting in the complete leaching of the core. The green-white precipitate formed during the course of the chemical reaction was filtered and dried. It was analyzed with XRD, which gave characteristic peaks of AgCl. Thus these reactions suggest that the shell is permeable to ions as well as molecules. Similar reaction was also observed in case of TiO_2 covered Ag clusters. When compared to silver, gold nanoparticles are less reactive to halocarbons. It took several hours for completion, leaving behind a blue precipitate, which became colourless in several days upon complete leaching of Au.

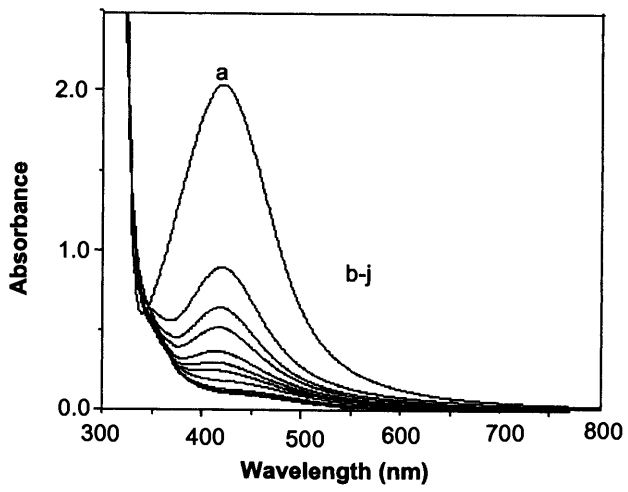

Fig. 4 Time dependence UV-Visible spectra of the reaction of $Ag@ZrO_2$ with benzyl chloride indicating the selective leaching of the metal core. Spectrum *a* was taken in the absence of the reactant and *b-j* in presence, at 10 minutes interval.

The halocarbon reaction of nanomaterials was also studied by voltammetry. For this study, 1 ml of benzyl chloride was added to a reaction mixture which contain about 4 ml of the colloidal solution and 10 ml of solvent-supporting electrolyte system. Typical time dependent superimposed CV obtained for $Ag@ZrO_2$ is shown in Fig. 5. Curve *a* shows the CV of $Ag@ZrO_2$ in the absence of benzyl chloride and *b* to *g* show the CV obtained at 10 minutes interval after adding benzyl chloride. With the addition of benzyl chloride, it is observed that both the characteristic anodic and cathodic peak current decreases (curves *b* to *h*) and finally it becomes flat, giving the original background current of Pt electrode in CH_3CN containing TBAHFP (curve *i*).

There is also some shift in the anodic peak potential towards negative values during the successive scans in which the value of ΔE_p decreases. This may be due to the decrease in E_{pa} values or change in the oxidation potentials of the redox system. It is to be noted that the decrease in the peak current is due to the removal of electro active Ag cores through the shell by halogens, leading to the precipitation of Ag as AgCl. A similar reaction with aliphatic halogens such as CCl_4 and $CHBr_3$ was also carried out under identical experimental

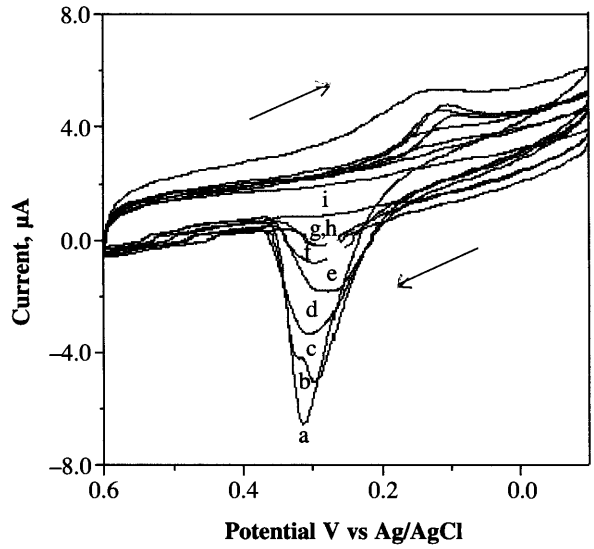

Fig. 5 Time dependent superimposed cyclic voltammograms of the reaction between $Ag@ZrO_2$ and benzyl chloride on Pt electrode in CH_3CN containing 0.1M tetrabutyl ammonium hexafluorophosphate (TBAHFP) at a constant sweep rate of 0.3 Vs^{-1}. The voltammetric curve a was taken in absence of reactant and b-i in presence, at 10 minutes interval.

conditions (with $Ag@ZrO_2$). Similar time dependent CV and UV-visible spectra were also obtained for the reaction between $Au@TiO_2$ and benzyl chloride. The rate of decrease in current for both anodic and cathodic peaks is not uniform unlike the reaction of Ag nanoparticles. A random shift of peak potentials with time is observed. The above studies confirm that ion transport is still possible through pores.

It is noted that ruthenium dye sensitized nanocrystalline–TiO_2 based semiconductor materials have been used in rapidly emerging solar energy technology. In order to see the efficient absorption of the dye molecule on the TiO_2 shell and to study the reactivity of the modified particles towards halocarbons, N3 dye (cis-dithiocyanato bis (2.2'bipyridyl 4,4' dicarboxylic acid) ruthenium(II)) was added to the cluster solution[19]. This dye has been used extensively in dye sensitized photovoltaic cells for several years. Partial blocking of the pores of the shell by the dye molecules was noted from the decrease in current in voltammetry, which became saturated at a particular concentration of dye. The core structure is stable with the addition of halocarbons showing effective absorption.

Alloy nanomaterials containing both Ag and Au nanoparticles and oxide covers were also synthesized and characterized. Three alloy compositions namely (A) Ag_2Au, (B) AgAu and (C) $AgAu_2$ were synthesized. Typical UV-Visible spectra of the alloy solutions are shown in the Fig. 6. With the increase in the composition of Au, the plasmon absorption was found to be shifted from 473 nm to 510 nm and further to 531 nm (red shift), which is indicative of the incorporation of Au. The absorption spectra confirm that these are alloys and not core-shell structures (Au over Ag or Au over Ag)[20].

Cyclic voltammograms were recorded in order to characterize these nanocomposite alloy materials based on their redox chemistry. Typical CVs of Ag_2Au (A) at different sweep rates are shown in Fig. 7. There are some shifts towards negative values in their peak potentials from the value of pure zirconium oxide coated Ag nanomaterials. At the sweep rate of 0.3 Vs^{-1}, the anodic peak (E_{pc}) is at 0.175 V and cathodic peak (E_{pa}) is at 0.005 V.

The calculated $E_{1/2}$ value for this alloy is 0.090 V with peak separation of (ΔE_p) 0.170 V. With the sweep rate of 0.3 Vs^{-1} (curve a) and 0.5 Vs^{-1} (curve b), the anodic peak potential and current do not increase appreciably. However, the cathodic peak current and peak potential increase linearly with scan rate. Similarly voltammograms were also recorded for the different alloys such as (B) and (C). There is not much difference in the $E_{1/2}$ values for the two alloys (B) and (C) from (A). However, the peak separation value (ΔE_p) decreases from 0.170 V to 0.075 V in case of alloy (B) and again increases to 0.95 V for (C) under the same sweep rate of 0.3 V s^{-1}. The exact reason for this difference is not known, but may be due to the change of the system from reversible to quasi-reversible state, by the addition of either of the components to the pure system.

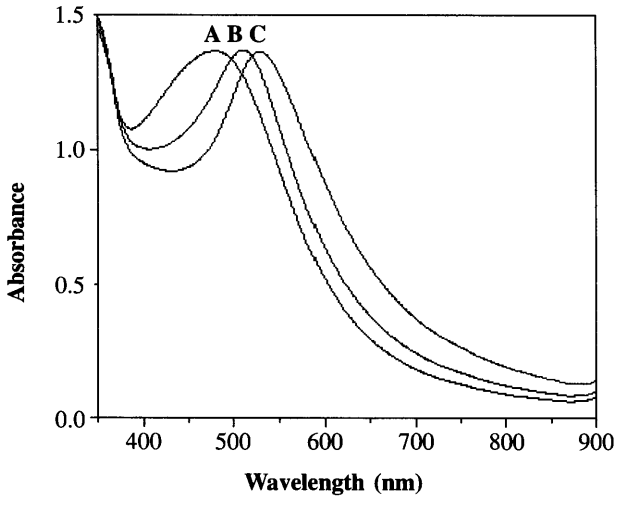

Fig. 6 UV-Visible spectra of alloy of zirconium oxide coated Au and Ag nanomaterials of different compositions (A) Ag_2Au_1, (B) AgAu and (C) $AgAu_2$

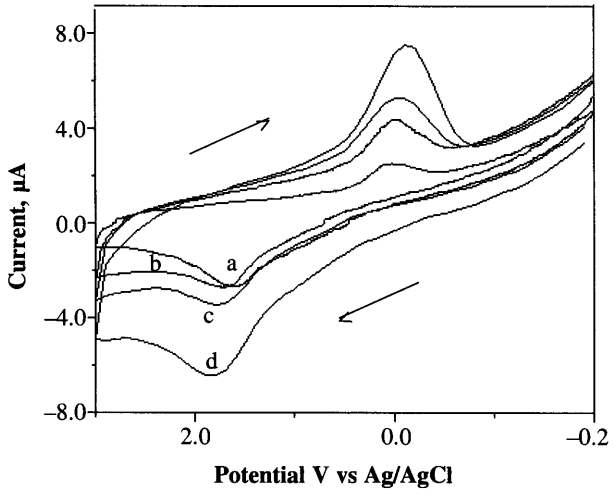

Fig. 7 Cyclic voltammograms for Ag_2Au (Alloy A) on Pt electrode in CH_3CN containing 0.1 M tetrabutylammonium hexafluorophosphate at different sweep rates in (V s^{-1}) a= 0.3 , b= 0.5 , c=0.7 and d=0.9.

Conclusion

Oxide covered Ag and Au nanoparticles have been prepared by one pot synthesis and have been investigated with cyclic voltammetry. The metal cores are still accessible to electron transfer reactions through the pores of the encapsulating shell. The pores can be blocked partially by adsorbates, but the cores are still reactive towards halocarbons. The metal cores can be completely destroyed by halocarbons and these reactions with nanoparticles may be important for their destruction and environmental decontamination. The reaction has been monitored by cyclic votammetry.

Acknowledgements

The last author (T P) acknowledges financial support from the Government of India, Ministry of Information Technology and the Space Technology Cell of Indian Institute of Technology, Madras. The authors (V S and RTT) are thankful to CSIR, New Delhi for the award of Research Associateship and Junior Research Fellowship respectively.

References

1 (a) A Takami, H Kurita and S Koda *J Phys Chem* B **103** (1999) 1226; (b) H Kurita, A Takami and S Koda *Appl Phys Lett* **72** (1998) 789

2 F Caruso *Adv Mater* **13** (2001) 11

3 A C Templeton, W P Wuelfing and R W Murray *Acc Chem Res* **33** (2000) 27

4 S Link and M A EI-Sayed *Int Rev Phy Chem* **19** (2000) 409; N Sandhyarani and T Pradeep *Int Rev Phy Chem* **22** (2003) 221

5 J J Storhoff and C Mirkin *Chem Rev* **99** (1999) 1849

6 C A Foss, G L Hornyak, J A Stockert and C R Martin *J Phys Chem* **98** (1994) 2963

7 V Kreibeig and M Vollmer Optical *Properties of Metal Clusters* Springer Berlin (1995)

8 (a) L M Liz-Marzan, M Giersig and P Mulvaney *Langmuir* **12** (1996) 4329; (b) L M Liz-Marzan, M Giersig and P Mulvaney *Chem Commun* (1996) 731

9 I P Santos, D S Koktysh, A A Mamedov, M Giersig, N A Kotov and L M Liz-Marzan *Langmuir* **16** (2000) 2731

10 (a) R T Tom, A Sreekumaran Nair, M Aslam, C L Nagendra, R Philip, K Vijayamohanan and T Pradeep *Langmuir* **19** (2003) 3439; (b) V Eswaranand and T Pradeep *J Mat Chem* **12** (2002) 2421

11 D P Dufaux and M R Zachatiah *Environ Sci Technol* **31** (1997) 2223

12 J Burdeniuc and R H Crabtree *Science* **271** (1996) 340

13 G Nicoll and J S Francisco *Environ Sci Technol* **33** (1999) 4102

14 Y C Chien, H P Wang and Y W Yang *Environ Sci Technol* **35** (2001) 3259

15 G Mie *Ann Physik* **25** (1908) 377

16 N K Chaki, S G Sudrik, H R Sonawane and K Vijayamohanan, *Chem Commun* (2002) 76

17 M Aslam, N K Chaki, I S Mulla and K Vijayamohanan *Appl Surf Sci* **182** (2001) 338

18 I P Santos and L M Liz-Marzen *Langmuir* **15** (2000) 948

19 K Kalyanasundaram and M Gratzel *Optoelectronic Properties of Inorganic Solids* (Eds: D M Roundhill and J P Fackler, Jr.) Plenum Press New York (1999) 169

20 Y Kim, R C Johnson, J Li, J T Hupp and G C Schatz *Chem Phys Lett* **352** (2002) 421